Integrative and Comparative Biology

Integrative and Comparative Biology, volume 62, number 6, pp. 1710–1724
https://doi.org/10.1093/icb/icac127
Society for Integrative and Comparative Biology

REEFS, CLIMATE CHANGE PAPER

Aquatic Walking and Swimming Kinematics of Neonate and Juvenile Epaulette Sharks

Marianne E. Porter[*,1], Andrea V. Hernandez[*], Connor R. Gervais[†,‡] and Jodie L. Rummer[†§]

[*]Department of Biological Sciences, Florida Atlantic University , 777 Glades Road, Boca Raton, FL 33431, USA; [†]ARC Centre of Excellence for Coral Reef Studies, James Cook University, Townsville, QLD 4811, Australia; [‡] Department of Biological Sciences, Macquarie University, Sydney, NSW 2109, Australia; [§]College of Science and Engineering, James Cook University, Townsville, QLD 4811, Australia

[1]E-mail: mporte26@fau.edu

Synopsis The epaulette shark, *Hemiscyllium ocellatum*, is a small, reef-dwelling, benthic shark that—using its paired fins—can walk, both in and out of water. Within the reef flats, this species experiences short periods of elevated CO_2 and hypoxia as well as fluctuating temperatures as reef flats become isolated with the outgoing tide. Past studies have shown that this species is robust (i.e., respiratory and metabolic performance, behavior) to climate change-relevant elevated CO_2 levels as well as hypoxia and anoxia tolerant. However, epaulette shark embryos reared under ocean warming conditions hatch earlier and smaller, with altered patterns and coloration, and with higher metabolic costs than their current-day counterparts. Findings to date suggest that this species has adaptations to tolerate some, but perhaps not all, of the challenging conditions predicted for the 21st century. As such, the epaulette shark is emerging as a model system to understand vertebrate physiology in changing oceans. Yet, few studies have investigated the kinematics of walking and swimming, which may be vital to their biological fitness, considering their habitat and propensity for challenging environmental conditions. Given that neonates retain embryonic nutrition via an internalized yolk sac, resulting in a bulbous abdomen, while juveniles actively forage for worms, crustaceans, and small fishes, we hypothesized that difference in body shape over early ontogeny would affect locomotor performance. To test this, we examined neonate and juvenile locomotor kinematics during the three aquatic gaits they utilize—slow-to-medium walking, fast walking, and swimming—using 13 anatomical landmarks along the fins, girdles, and body midline. We found that differences in body shape did not alter kinematics between neonates and juveniles. Overall velocity, fin rotation, axial bending, and tail beat frequency and amplitude were consistent between early life stages. Data suggest that the locomotor kinematics are maintained between neonate and juvenile epaulette sharks, even as their feeding strategy changes. Studying epaulette shark locomotion allows us to understand this—and perhaps related—species' ability to move within and away from challenging conditions in their habitats. Such locomotor traits may not only be key to survival, in general, as a small, benthic mesopredator (i.e., movements required to maneuver into small reef crevices to avoid aerial and aquatic predators), but also be related to their sustained physiological performance under challenging environmental conditions, including those associated with climate change—a topic worthy of future investigation.

Introduction

Coral reefs and the organisms that they support can experience dramatic environmental changes over diel cycles, but are also under threat due to climate change-induced increases in temperature and carbon dioxide (CO_2), and decreases in oxygen (O_2). Despite this, some species, like the epaulette shark (*Hemiscyllium ocellatum*), seem to thrive. Long-tailed carpet sharks (family Hemiscylliide, comprising two genera, *Chiloscyllium* and *Hemiscyllium*) are small, benthic sharks that occupy tropical reefs in the Indo-West Pacific Ocean (Compango et al. 2005; Heupel and Bennett 2007; Allen et al. 2016). Epaulette sharks around Heron Island in the southern Great Barrier Reef exhibit small home ranges with population sizes modeled to be anywhere from 550 to 2200 individuals (Heupel and Bennett 2007). The

Advance Access publication July 27, 2022

genus *Hemiscyllium* is made up of nine species (i.e., including the epaulette shark) that use their paired pectoral and pelvic fins to walk along the benthos or between coral reef flat tidepools as they become isolated and exposed with the outgoing tide (Dudgeon et al. 2020). In doing so, walking sharks routinely experience dramatic fluctuations in temperatures, CO_2, and O_2 (Pridmore 1994; Routley et al. 2002; Chapman and Renshaw 2009; Harborne 2013; Heinrich et al. 2014; Nay et al. 2020) and, as such, have been emerging as a model species to understand the effects of climate change stressors on marine fishes.

Epaulette sharks and perhaps other similar small, benthic species appear to be physiologically resilient over acute and longer-term exposure to some but not all challenging environmental conditions (Rosa et al. 2017; Pereira Santos et al. 2021; Rummer et al. 2022). Not surprisingly, when epaulette sharks are experimentally exposed to near-future CO_2 conditions for more than 60 days, they maintain metabolic performance, hypoxia tolerance, and various feeding and shelter-seeking behaviors (Heinrich et al. 2014, 2015). Such findings are in line with those on the closely related tropical, white-spotted bamboo shark (*Chiloscyllium plagiosum*), where neither cellular damage nor effects on growth, development, or swimming have been noted under climate change-relevant CO_2 conditions (Lopes et al. 2018; Pegado et al. 2018, 2019). The epaulette shark has also been shown to tolerate hypoxia and anoxia (i.e., low to zero O_2 conditions) with metabolic depression and increased reliance on anaerobic pathways (Routley et al. 2002; Chapman and Renshaw 2009). However, when epaulette shark embryos are reared under future temperature scenarios, they develop faster, deplete their yolk more rapidly, and hatch earlier and smaller with altered coloration patterns and higher metabolic costs when compared to their current-day counterparts (Gervais et al. 2016, 2018; Wheeler et al. 2021). Indeed, there may be limitations to their physiological tolerance, and perhaps especially during early life stages (Gervais et al. 2016, 2018; Wheeler et al. 2020, 2021), such that other strategies like movement (i.e., to more favorable conditions) may be required (Gervais et al. 2018; Nay et al. 2020). Therefore, studying the link between locomotion and the physiological mechanisms required to tolerate challenging environmental conditions represents an essential next step in understanding how this group of important meso-predators will respond to future ocean conditions.

Despite being a good model for studying physiological responses to climate change, very few studies have examined epaulette shark kinematics: those that have only focused on adult life stages (Pridmore 1994; Goto et. al. 1999; Raoult et al. 2018). While ecological studies suggest that epaulette sharks walk from the moment they emerge from the egg, no study to date has specifically examined locomotion during early life stages (West and Carter 1990; Goto et al. 1999). Investigating how locomotor performance changes over the course of early ontogeny—perhaps the most vulnerable life stages, in terms of predator–prey interactions and environmental stressors (Gervais et al. 2016, 2018; Wheeler et al. 2021)—can offer insights into the kinematic mechanisms that allow animals to compensate for constraints (e.g., variations in size and muscle mass) to meet locomotor and ecological demands, especially under challenging environmental conditions. Body size and shape, tissue differentiation, maturation of sensory-motor systems, and ecological pressures (e.g., predation, foraging, habitat quality, and environmental conditions) all vary over ontogeny and can influence species' locomotor performance and therefore survival (Carrier 1996; Horning and Trillmich 1997; Herrel and Gibb 2006; Kirkton and Harrison 2006). Given that locomotor performance may be key to the epaulette sharks' robust response to challenging environmental conditions, we aimed to investigate how kinematics (i.e., walking and swimming) change over early ontogeny.

Here, we synthesize previous conservation physiology studies on the epaulette shark, examine the impacts of shape on neonate and juvenile kinematics, and make a case that this species is emerging as a powerful model organism to study the changing climate of coral reefs. We hypothesized that the changing shape of epaulette sharks during early ontogeny would affect the efficiency of their locomotor performance. While In ovo, epaulette shark embryos are nourished by their yolk sac, which is internalized during the final stages of development (Müller 1848; West and Carter 1990; Ballard et al. 1993; Rodda and Seymour 2008). Upon hatching, the internal yolk sac exclusively nourishes the neonate for several weeks (i.e., depending on temperature; Gervais et al. 2018; Wheeler et al. 2021). During this time, the yolk that the neonate sharks are storing creates a bulge in their abdomens that starts to diminish as neonates develop into juveniles (Fig. 1). As the yolk is depleted, the shark begins to actively forage for worms, crustaceans, and small fishes to supplement its nutritional intake (Stewart and Castillo 1984; Ballard et al. 1993; Heupel and Bennett 1998; Harahush et al. 2007). Therefore, we compared newly hatched neonates that are still carrying their yolk sac for endogenous nourishment to the more slender juveniles that have just begun to actively forage for food. We quantified axial body kinematics (velocity, tail beat amplitude and frequency, and body curvature) and axial body bending, fin rotation and duty factor, and tail kinematics for neonate and juvenile epaulette sharks during each of three sub-

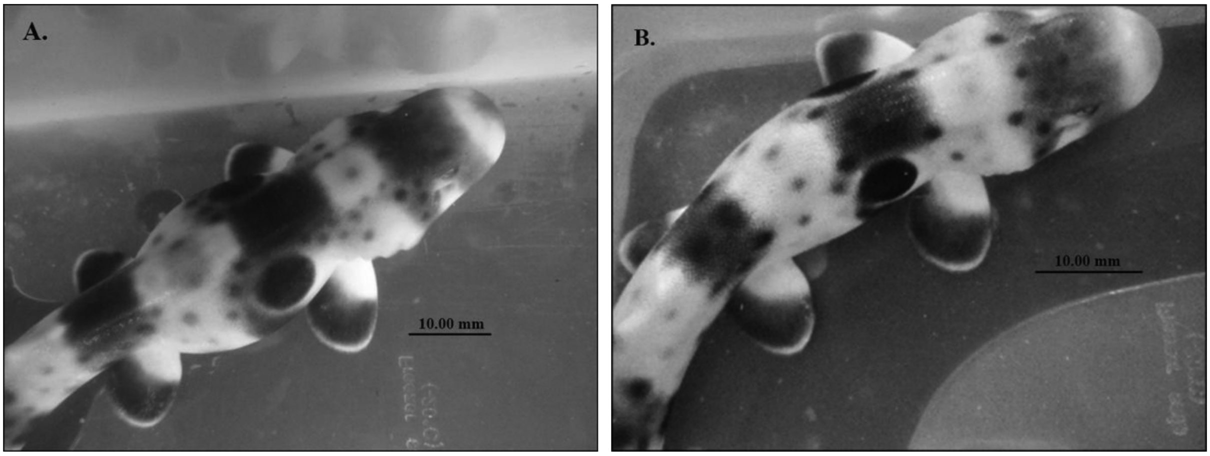

Fig. 1 Neonate (**A**) and juvenile (**B**) epaulette sharks. Note the bulbous abdomen shape in the neonate compared to the slender abdomen in the juvenile.

merged gaits that epaulette sharks use, including slow-to-medium walking (STMW), fast walking (FW), and swimming (SWIM) (Pridmore 1994). We predicted, *a priori*, that neonate kinematics would be different from juveniles because their more rounded shape could alter the axial undulations that power both submerged walking and swimming and restrict pectoral and pelvic girdle and fin rotations that would normally provide forward propulsion. Findings from this study will contribute to understanding the energetic costs of these kinematic variables over development, which may be linked to or represent trade-offs when these and other related species encounter the challenging environmental conditions predicted in future oceans.

Methods

Animal collection and care

All animal care and experimental protocols were approved by James Cook University Animal Ethics Committee regulations (permit: A2089, approved for this study) according to the Australian Code of Practice for the Care and Use of Animals for Scientific Purposes, and the Queensland Animal Care and Protection Act, 2001.

Neonate ($n = 6$) and juvenile ($n = 6$) epaulette sharks ($n = 12$ animals total) were collected, as eggs, from Sea World, Gold Coast, and housed and videoed in individual glass aquaria (50 cm × 27 cm × 24 cm) at the Marine and Aquaculture Research Facilities at James Cook University, Queensland, Australia. Upon hatching, neonates were maintained for up to 1 month, during which time they fed exclusively on their internal yolk sac, which has been reported to support their nutrition for up to five weeks depending on the temperature (West and Carter 1990; Payne and Rufo 2012; Gervais et al. 2018; Wheeler et al. 2021). For this study, neonates were characterized by the presence of their internal yolk sac and rejection of food offerings at 15 and 25 days post-hatching, but once animals began accepting food (approximately 30 days post-hatch), they were classified as juveniles (Gervais et al. 2018; Fig. 1). Neonate mass ranged from 7.66 to 17.10 g, and length ranged from 15.81 to 18.23 cm. Juveniles were fed bait pilchard (white meat only) and squid mantle every other day (see Gervais et al. 2018). Juvenile mass ranged from 15.86 to 27.95 g, and length ranged from 18.71 to 22.53 cm.

In addition to using mass and length to determine how ontogeny influences locomotor performance, we made several other calculations (Table 1). We used fineness ratio (animal total length/width; widest point of the abdomen) as a two-dimensional approximation of body shape to quantify the impacts of retaining an internal yolk sac on locomotor performance. We used the widest point of the abdomen to model the body as a cylinder to calculate the second moment of area (cm^4), a structural predictor of stiffness, of the body (Porter, Roque and Long 2009, 2011). Finally, we used animal length and mass to calculate the body's mass moment of inertia ($g\ cm^2$), which estimates a body's ability to resist rotational acceleration around an axis (Porter, Roque and Long 2009, 2011).

Gaits

Three submerged gaits have been defined for adult epaulette sharks, including two walking gaits and one swimming gait (Pridmore 1994). The slower of the two walking gaits, (STMW, $<4.5\ cm\ s^{-1}$), includes a symmetrical walking-trot with diagonal-sequence stepping and a standing wave down the body produced by lateral bending along the body axis, pectoral and pelvic fin rotation about their respective girdles, and low pec-

Table 1 Body shape and kinematic variables

	Variable	Units	Definition	Points tracked
Body shape variables	Body width	g	Widest point of abdomen	–
	Body total length	cm	Tip of head to tip of caudal fin	–
	Fineness ratio	–	Two-dimensional shape description	length/width
	Second moment of area	cm^4	Ability of body to resist bending, modeled as a circle	$(\pi(\text{width}/2)*4)/4$
	Mass moment of inertia	$g\ cm^2$	Ability of body to resist rotational acceleration	$(m*TL^2)/32$
Kinematic variables	Velocity	$cm\ s^{-1}$	Body displacement over time	2
	Tailbeat frequency	Hz	Tailbeat cycles over time	5
	Tailbeat amplitude	cm	Peak-to-peak distance during a complete later excursion	5
	Duty factor	%	Time fin is in contact with substrate over the total duration of the stride	8, 9, 12, 13
	Axial bending	°	Body bending in the anterior, middle, and posterior region	≯123, ≯234, ≯345

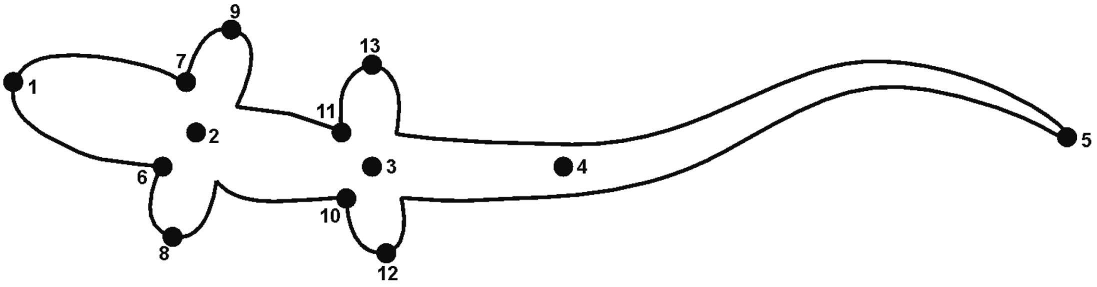

Fig. 2 Thirteen anatomical landmarks were tracked over time in Logger Pro to provide the raw x–y-coordinate data used to calculate the kinematics of the three gaits. Five points were placed along the body midline from the most anterior tip (the snout; point 1) to the most posterior tip (tip of the tail; point 5). The remaining eight points were made along the leading edge of each pectoral and pelvic fin (points 6, 7, 8, 9, 10, 11, 12, 13).

toral and pelvic fin step frequency. FW (4.5–8 $cm\ s^{-1}$), which is considered a transitional gait from walking to swimming, includes a distinct traveling-wave down the body that is produced by lateral bending along the body axis, fin rotation about their girdles, and high pectoral and pelvic fin step frequency. The fastest gait, (SWIM, $\sim$26 $cm\ s^{-1}$), is characterized by a traveling wave down the body that is produced by lateral bending of the body axis but no fin interaction with the substrate. In this study, we found that neonates and juveniles exhibited all three of these documented locomotor gaits at speeds within the ranges previously reported (Pridmore 1994).

Video recordings and analyses

While sharks were in their individual tanks, video recordings were made using a GoPro Hero 3 + Black (GoPro, Inc., USA) using a standard narrow field of view, 1080p and 30fps settings, located 15 cm below the tank, for a ventral view. These non-linear field of view settings minimize wide angle distortion and parallax. Using iMovie (Apple Inc, Cupertino, CA, United States), video recordings were separated into 3–5 s clips, where straight walking or swimming across the tank was clearly observed. For each shark ($n = 12$), one video clip of each of the three gaits was analyzed, resulting in six video clips for each gaeit for each neonate and six video clips for each gait for each juvenile ($n = 36$ total videos). Each STMW video consisted of 5.6 mean step cycles (range: 3–10), while each FW video contained 5.4 cycles (range: 3–7). Swimming videos contained a mean of 3 tailbeats (range: 2–5). The video clips were used to track 13 anatomical landmarks through time using a data-collection and analysis software (Logger Pro, Vernier), thus providing raw x–y-coordinate data to calculate the characteristic movements of the three gaits (Fig. 2). Five points were placed along the body midline from the most anterior (snout; 1) to the most posterior (tip of caudal fin; 5) parts of the body but including points on the mid-line along the pectoral (2) and pelvic (3) girdles, as well as the base of the caudal fin (4). The remaining eight points (6, 7, 8,

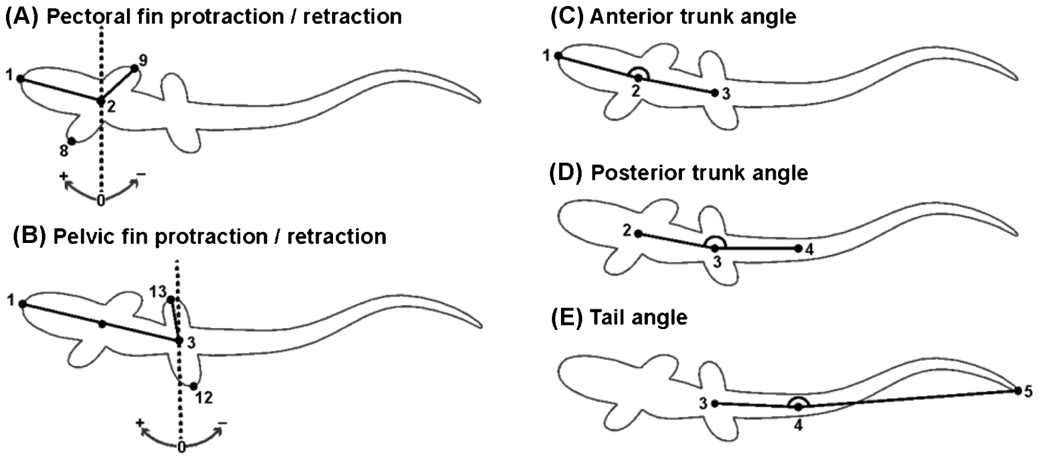

Fig. 3 Bending angles of fins and the shark body. Pectoral (**A**) and pelvic (**B**) fin rotation angles. These angles were normalized by the resting angle, the angle when the fin was neither protracting nor retracting, to determine the degree (°) of protraction (+) and retraction (-) in the fins. Axial bending (**C**, **D**, and **E**) was calculated for the anterior portion (**C**) of the trunk as ∡123, the posterior portion (**D**) of the trunk as ∡234, and for the tail (**E**) as ∡345. These angles were then normalized by 180° to determine the degree (°) of lateral bending from a straight-line position in the body midline.

9, 10, 11, 12, 13) were made along the leading edge of each fin.

Kinematic variables

In order to quantify the kinematics of the neonates and juveniles, six variables were calculated from the raw data provided by Logger Pro. Velocity (cm s^{-1}) was measured from the point closest to the center of mass (2) and was calculated as the displacement of this point over time (Table 1). Tail beat frequency (Hz) was measured as the number of cycles over time. Tail beat amplitude (cm) was measured for the tip of the tail (5) as the peak-to-peak distance covered from one lateral extension to another (Hoffmann et al. 2017; Porter et al. 2020). Duty factor (%) was measured using the most distal points of the anterior edge of the fins (8, 9, 12, 13) and calculated as the ratio between the duration of the contact interval (s) to the total duration of the stride cycle (Table 1). Pectoral and pelvic fin angles (Fig. 3A and B) were calculated from the angles (°) created between the tip of the snout (1), the midpoints along the pectoral (2) and pelvic (3) girdles, and the most distal points of the anterior edge of the fins (8, 9, 12, 13). The apex of each angle is the midpoint of either the pectoral and pelvic girdles (points 2 and 3), which are along the body midline, thus allowing us to measure angles near each girdle. These angles were then normalized by their resting angle, the angle when the fin was neither protracting nor retracting (STMW: 117.7° ± 1.4, FW: 120.7° ± 2.02, SWIM: 108.7° ± 4.71), to determine the degree (°) of protraction and retraction in the fins. These angles were then smoothed using a Gaussian filtering in MATLAB_R2018a (The MathWorks, Inc., Natick, MA, USA). Axial bending was calculated for the anterior portion of the trunk from the angles (°) created between the tip of the snout (1) and the midpoints along the pectoral (2) and pelvic (3) girdles (Fig. 3C, D, and E; Table 1). Axial bending in the posterior portion of the trunk was calculated from the angles (°) created between the midpoints along the pectoral (2) and pelvic (3) girdles, and the midpoint of the proximal base of the tail (4). Axial bending for the tail was measured from the angles (°) created between the midpoint of the pelvic (3) girdle, the base of the tail (4), and the tip of the tail (5). These angles were then normalized by their resting angle (180°) to determine the degree (°) of lateral bending from a straight-line position in the body midline. The angles were then smoothed using a Gaussian filtering in MATLAB_R2018a similar to pectoral and pelvic fin angles.

Statistical analyses

We examined differences in body shape between neonates and juveniles (length, mass, fineness ratio, second moment of area, mass moment of inertia) with *t*-tests using JMP 11 (SAS, Cary, NC, USA). The differences in kinematic variables (velocity, tailbeat frequency, tailbeat amplitude) were analyzed for statistical significance in JMP using mixed effects models, and the main effects included life stage, gait, and fineness ratio to account for individual differences in body shape. Axial bending was examined using a mixed model with life stage, gait, fineness ratio, and position (anterior, posterior, and tail) as main effects. Duty factor was evaluated in a model using life state, gait, fineness ratio, and fin (pectoral or pelvic) as main effects. For each action (i.e., protraction and retraction), we examined fin rotation

Table 2 Summary of body shape variables for neonate and juvenile epaulette sharks.

Variable	Neonate	Juvenile
Width (cm)	1.47 ± 0.83	1.58 ± 0.06
Length (cm)∗	16.66 ± 0.39	20.80 ± 0.53
Mass (g)∗	12.13 ± 1.43	22.91 ± 1.78
Fineness ratio	11.48 ± 0.65	13.19 ± 0.42
Second moment of area (cm^4)	0.25 ± 0.05	0.32 ± 0.04
Mass moment of inertia ($g\ cm^{\ 2}$)∗	0.11 ± 0.02	0.32 ± 0.04

All values are mean ± SEM. Significant differences (P <0.05) are indicted with an ∗ by each variable.

using a mixed model with life stage, gait, fineness ratio, and fin (pectoral or pelvic) as main effects. *Post-hoc* differences were determined using Tukey's tests. Figures show data from significant effects. A summary of kinematic variables is provided in Table 1.

Results

Body shape

The neonates used in this study were 20% shorter ($F_{1,10} =$ 39.28, $P < 0.0001$) and weighed 47% less ($F_{1,10} = 22.22$, $P = 0.0008$; Table 2, Fig. 4B and C) than the juveniles. Neither body width nor second moment of area differed between neonates and juvenile epaulette sharks (Fig. 4). The fineness ratio, a two-dimensional description of shape, was 18% less in neonates compared to juveniles but was not significant ($F_{1,10} = 4.87$, $P = 0.0519$, Fig. 4D). Finally, the mass moment of inertia was three times lower in neonates when compared to juvenile sharks ($F_{1,10} = 25.88$, $P = 0.0005$, Fig. 4F).

Velocity

Velocity varied significantly ($F_{4,31} = 20.26$, P <0.0001), and gait was the only significant effect in the model ($P <$ 0.0001, Fig. 5; Table 3). Velocity increased among gaits from slow-to-medium walking (STMW), fast walking (FW), and swimming (SWIM). The mean velocity during SWIM (11.68 cm s^{-1}) was nearly twice as fast as during FW (6.68 cm s^{-1}), and velocity during FW was more than twice what was quantified during STMW (3.02 cm s^{-1}).

Tailbeat frequency and amplitude

Tailbeat frequency did not vary significantly when examining life stage, fineness ratio, and gait as main effects (Fig. 6A, point 5; Table 3). However, the tailbeat amplitude model was significant ($F_{4,31} = 2$, $P = 0.048$; Fig. 6B), and none of the main effects was significant.

Axial bending

The axial bending model was significant ($F_{6,101} = 21.33$, $P < 0.0001$, Fig. 7; Table 3); position along the body (anterior, posterior, and tail) was the only significant effect ($P < 0.0001$). The degree of axial bending increases from anterior trunk to tail, and the tail angle is nearly three times greater than the anterior bending angle.

Duty factor

The duty factor varied significantly ($F_{4,43} =$ 5.7061, $P = 0.0009$), and gait ($P = 0.0016$) and fin ($P = 0.0068$) were significant effects (Fig. 8). On average, fins were in contact with the substrate 5% longer during STMW than during FW, and overall pelvic fins were in contact with the floor 5% longer than pectoral fins. The duty factor was similar between neonates and juveniles. The SWIM gait was not included in this statistical model because neither pectoral nor pelvic fins are in contact with the bottom of the tank during this gait.

Fin rotation

The fin protraction model was significant ($F_{5,64} = 35.46$, $P < 0.001$, Fig. 9A; Table 3), and gait and fin were significant effects ($P = 0.0464$ and $P < 0.0001$, respectively). Significantly more fin protraction occurred during STMW when compared to SWIM, while FW was intermediate. There was three times more pelvic protraction than pectoral protraction. The fin retraction model was significant ($F_{5,64} = 20.56$, $P < 0.001$, Fig. 9B), and age, gait, and fin were all significant main effects ($P = 0.0085$, $P = 0.0111$, and $P < 0.0001$, respectively). Specifically, neonates had significantly more fin retraction than juveniles, and fin retraction was four times greater in pelvic fins when compared to pectoral fins. Significantly more fin retraction occurred during STMW gaits when compared to SWIM, while FW was intermediate.

Discussion

We examined the impacts of ontogeny (i.e., shape variations) on the kinematics of neonate and juvenile epaulette sharks (*H. ocellatum*), a coral reef species that has been used since the early 2000s to understand physiological mechanisms underpinning tolerance to future ocean conditions (reviewed in Pereira Santos et al. 2022 and Rummer et al. 2022). Epaulette sharks are documented to utilize three locomotor gaits, which we also observed in both neonates and juveniles. However, given that neonates emerge from their eggs with bulbous yolk sacs that are maintained for up to 5 weeks, we expected their locomotion to be markedly different from the slender, actively foraging juveniles. We

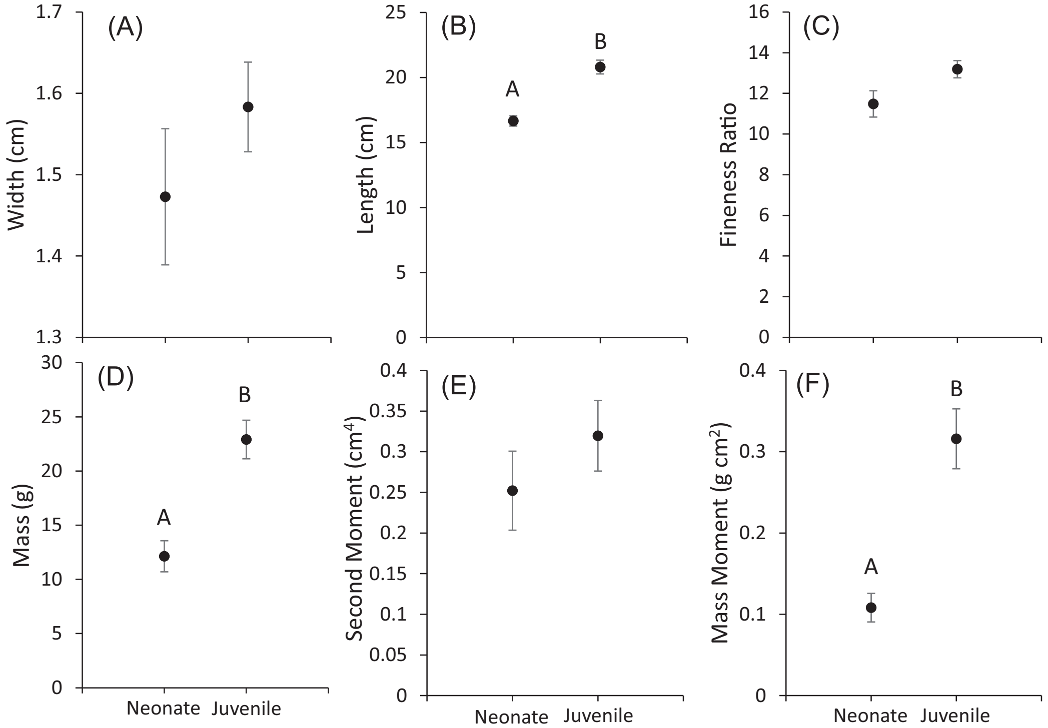

Fig. 4 Body metrics and shape. Juveniles had significantly greater length, mass, and mass moment of inertia compared to neonates. Values shown (circle) are the means. Error bars indicate ± SEM. *Post hoc* statistical differences among groups are denoted with differing letters above each.

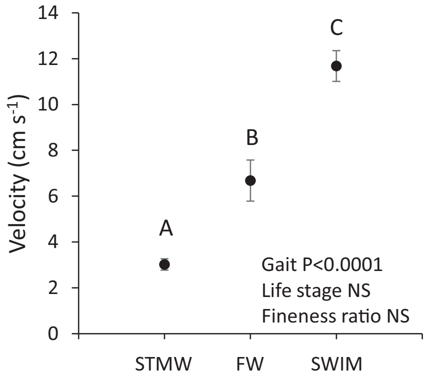

Fig. 5 Velocity (cm s^{-1}) of the approximate center of mass (point 2) vs. gaits. Velocity varied in whole model statistics and gait was the only significant effect. Since velocity did not change among life stages, values shown here are means (circles) from neonates ($n = 6$) and juveniles ($n = 6$). Using Tukey *post hoc* comparisons, we found that velocity increased among gaits from STMW, FW, and SWIM. Error bars indicate ± SEM. *Post hoc* statistical differences among groups are denoted with differing letters above each.

hypothesized that the larger and rounder abdomen and resulting different shape of neonates would, specifically, decrease the fineness ratio and increase the second moment of area, as well as restrict the fin rotations that provide significant forward propulsion during both submerged walking gaits. We also predicted that the body shape of neonates would result in alterations in the axial undulations that power both submerged walking and swimming. However, we found few differences in kinematic variables or body shape metrics between neonates and juveniles, thus refuting our original hypotheses.

Of course, neonates and juveniles were inherently different in size, which would be expected. Yet, while length (cm) and mass (g) varied between these life stages, there were no significant differences in fineness ratio, a two-dimensional shape metrics, or second moment of area (cm^4), a structural predictor of body stiffness (Fig. 4; Table 2). However, we did find that mass moment of inertia, which is used to quantify angular acceleration (g cm^2) around an axis, was greater in juvenile sharks. While we expected velocity (cm s^{-1}) and axial bending angle (°) to differ among these gaits, which it did, there were no differences between life stages (Figs 5 and 7; Table 3). During the slowest walking gait, (i.e., STMW), the pelvic fins were in contact with the substrate for significantly longer than the pectoral fins, and duty factor (i.e., the time the fin was in contact with the substrate; %) did not vary between life stages (Fig. 8). Neither life stage nor fineness ratio significantly affected fin protraction (°), but we found significant effects from both gait and fin (pectoral or pelvic) (Fig. 9). Specifically, the most fin protraction occurs in the pelvic fins during the STMW gait. Similarly, the most fin

Table 3 Summary of kinematic variables for neonates and juveniles across all three gaits.

		Neonate			Juvenile		
Variable		**STMW**	**FW**	**SWIM**	**STMW**	**FW**	**SWIM**
Velocity (cm s^{-1})		2.712 ± 0.22	6.98 ± 1.67	11.47 ± 0.79	3.33 ± 0.431	6.38 ± 0.84	11.9 ± 1.16
Tailbeat	Frequency (Hz)	2.49 ± 1.40	1.34 ± 0.014	1.84 ± 0.09	0.754 ± 0.25	1.52 ± 0.18	1.30 ± 0.28
	Amplitude (cm)	0.50 ± 0.10	1.14 ± 0.14	1.53 ± 0.19	1.48 ± 0.72	1.48 ± 0.20	1.87 ± 0.18
Duty factor (%)	Pectoral	54.71 ± 1.21	51.38 ± 3.57	–	50.56 ± 1.90	45.58 ± 3.95	–
	Pelvic	57.50 ± 0.68	51.66 ± 1.40	–	59.42 ± 1.74	51.88 ± 1.65	–
Axial bending (°)	Anterior	9.49 ± 0.91	10.16 ± 0.90	10.17 ± 1.15	6.58 ± 0.65	9.09 ± 0.89	8.47 ± 0.93
	Posterior	16.68 ± 1.11	20.65 ± 3.09	15.61 ± 1.66	15.67 ± 1.57	14.91 ± 1.18	17.21 ± 1.96
	Tail	15.43 ± 1.37	21.95 ± 2.15	26.51 ± 1.87	20.45 ± 3.17	25.00 ± 2.12	25.72 ± 3.17
Fin rotation (°)	Pectoral protraction	8.39 ± 2.03	11.68 ± 2.48	10.17 ± 3.17	5.36 ± 1.59	6.83 ± 2.27	7.07 ± 1.62
	Pelvic Protraction	37.96 ± 1.17	31.85 ± 6.53	26.43 ± 3.40	35.69 ± 2.66	29.29 ± 4.43	22.36 ± 1.26
	Pectoral retraction	−9.89 ± 2.18	−10.33 ± 1.56	−8.14 ± 1.45	−4.74 ± 0.93	−3.95 ± 1.49	−6.00 ± 1.90
	Pelvic retraction	−36.50 ± 3.38	−33.82 ± 7.17	−24.38 ± 2.55	−31.48 ± 1.74	−27.62 ± 2.65	−20.65 ± 2.77

All values are mean ± SEM.

retraction (°) also occurs in the pelvic fins during the STMW gait, which was notably the greatest during the neonate life stage. These findings suggest that submerged locomotion in neonates is not impacted by the yolk sac and the effects it has on body shape, as all aspects of submerged locomotion were comparable to that of the juveniles. Future studies quantifying a greater number of individuals over a wider size ranges may capture the impacts of shape on walking and swimming kinematics of this species.

Body shape

We found significant differences between neonate and juvenile epaulette sharks in body length, mass, and mass moment of inertia, as expected, but body width, fineness ratio, and second moment of area were similar between these two life stages (Fig. 4; Table 2). The fineness ratio does trend toward the juvenile sharks having a longer and more slender two-dimensional body shape when compared to the neonates with their bulbous yolk sac. Perhaps body shape differences would be more pronounced if neonates were compared to later stage juveniles or sub-adults. Indeed, future studies could examine animals with a wider range of sizes to truly appreciate ontogenetic shape changes in this species. Also of note, the mass moment of inertia was significantly greater in the juveniles, suggesting that this body shape metric might also be relevant when studying maneuverability, rather than the linear movements examined here (Porter, Roque, and Long 2011). Epaulette sharks live in complex coral reef habitats, and the ability to effectively maneuver and the associated energetic costs under different environmental conditions would be an important aspect of their locomotion to explore in future studies.

Body shape can impact performance in fishes. Despite having a similar fineness ratio (i.e., two-dimensional shape) to leopard sharks (*Triakis semifasciata*), epaulette sharks are able to produce tighter turns due to their long caudal fins (Porter, Roque, and Long 2009). When the caudal fin was removed from the turn analyses, however, leopard sharks and epaulette sharks produced similarly tight turns. Long et al. (2010) proposed that fish change their shape, or the way the body would interact with the flow of water, over several time scales. While swimming, fish can change their shape using a propulsion generating wavelength, which is termed undulatory body reconfiguration. However, fish can also use behaviors to change their shape, such as during a turning maneuver, which is termed postural body reconfiguration. Both of these types of body reconfigurations are transient, occurring over the smallest time scales, such as during a tailbeat or turning maneuver. A third type—form reconfiguration—occurs

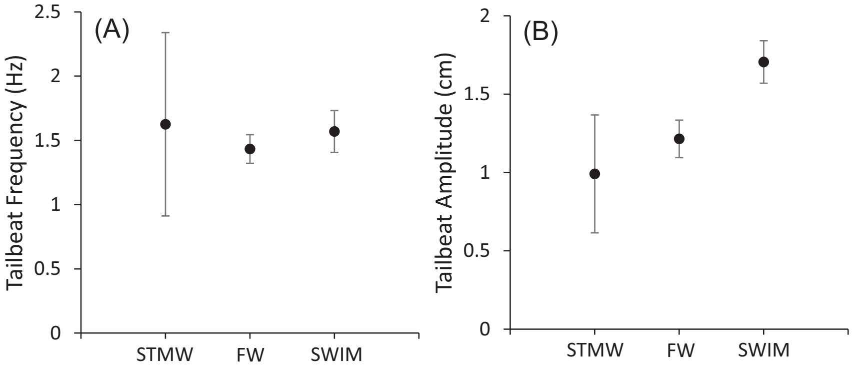

Fig. 6 Tailbeat kinematics. (**A**) Tailbeat amplitude did not vary with life stage, gait, or fineness ratio. (**B**) The whole model for tailbeat amplitude was significant, but none of the main effects was significant; however, amplitude trends increase among the gaits and are greatest during SWIM. Means (circle) are shown for each gait. Error bars indicate ± SEM.

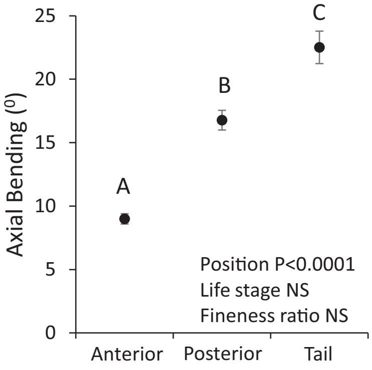

Fig. 7 Axial bending during all three gaits. The whole model showed significant differences in axial bending, and position along the body (anterior, posterior, and tail) was the only significant effect. The degree of axial bending increases from anterior trunk to tail. The means (circles) shown are data for each angle that was pooled together from both age groups and from all gaits. Error bars indicate ± SEM. *Post hoc* statistical differences among groups are denoted with differing letters above each.

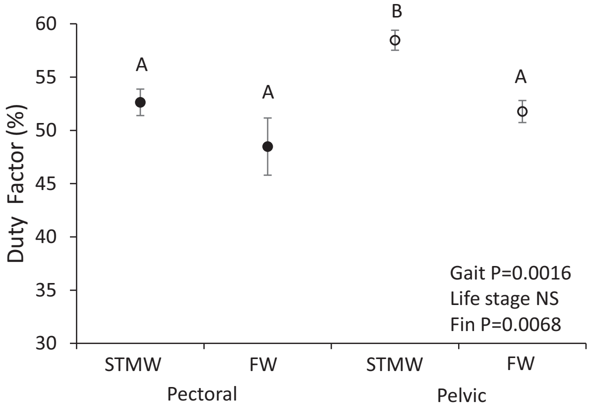

Fig. 8 Duty factor (%) of fin stride moving from protracted to retracted for pectoral (solid circle) and pelvic (open circle) fins at each walking gait. Duty factor did not differ between neonates and juveniles, but did vary in the pelvic fins only between gaits. On average, fins are in contact with the substrate 5% longer during STMW than during FW, and overall pelvic fins were in contact with the floor 5% longer than pectoral fins. Means are shown as circles. Error bars indicate ± SEM. *Post hoc* statistical differences among groups are denoted with differing letters above each.

over the largest temporal scale and is when the body changes in size or anatomical shape, such as in this study as epaulette sharks develop from neonate to juvenile stages. Given that form reconfiguration can occur within one generation (i.e., over ontogeny, developmental acclimation) or over many generations (i.e., transgenerational acclimation or adaptation), this would be a key concept to investigate in conjunction with mechanisms for coping with challenging environmental conditions, such as those experienced by the epaulette sharks.

Velocity and axial bending

Epaulette sharks' velocity differed depending on gait, not surprisingly; but velocity did not differ between life stages or with body fineness ratio (Fig. 5; Table 3). On average, velocity doubled between two submerged walking gaits (i.e., STMW to FW), but SWIM velocity was nearly double that of FW. Yet, epaulette sharks' average walking velocities (STMW: 3.02 cm s^{-1}; FW: 6.68 cm s^{-1}) were in the range to observe diagonal-sequence walking in epaulette sharks (Pridmore 1994). Quadrupeds, in general, can achieve efficient diagonal-sequence walking by implementing axial undulations that stabilize the animal's body (Hildebrand 1980; Hidlebrand 1989; Pridmore 1994; Ashley-Ross and Bechtel 2004; Reilly et al. 2006). The kinematics of the epaulette sharks in this study were quantified while animals were submerged in water where they would benefit from buoyant forces; although, it is important to note that elasmobranchs are generally negatively buoyant (Rosenblum et al. 2011). Stability is perhaps a larger

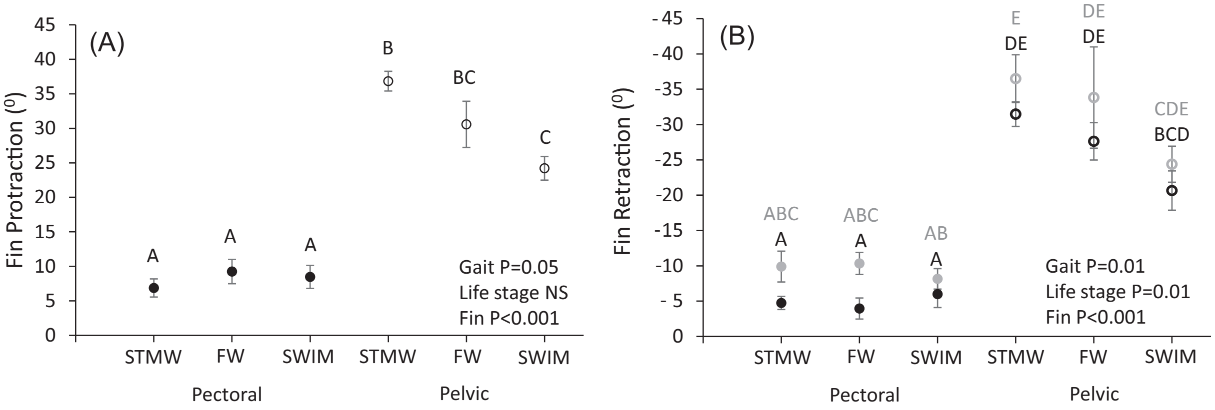

Fig. 9 Fin rotation varies among gaits and between fins. (**A**) In protraction, the whole model was significant, and gait and fin were significant effects. Pelvic fins (open circles) protracted significantly more than pectoral fins (closed circles). Significantly more fin protraction occurred during STMW compared to SWIM, while FW was intermediate. (**B**) In retraction, the whole model was significant, and life stage, gait, and fin were all significant main effects. Neonates (gray) had significantly more fin retraction compared to juveniles (black), and pelvic fin retraction was four times that of the pectoral fins. The gradient among gaits was observed in retraction. Error bars indicate ± SEM. *Post hoc* statistical differences among groups are denoted with differing letters above each.

issue when examining locomotion in terrestrial or transitional (water-to-land or land-to-water) environments. Examining the STMW and FW gaits in epaulette sharks out of water, as Pridmore (1994) did, may have resulted in significant differences among life stages in this study. Based on all of this information, larger animals would have longer stride lengths and move faster than smaller animals. Surface complexity would also be an important factor to consider when examining velocity. Travis (2020) calculated velocity in sub-adults walking whilst fully submerged or partially submerged, and reported significant differences between these conditions. In contrast, animals in this study were investigated whilst moving on a flat surface, but the complex reef structure and topography of the benthos could result in different outcomes. Indeed, the epaulette shark inhabits the complex matrix of coral reefs, such as those found within the Great Barrier Reef; therefore, examining their kinematics on complex surfaces would be more representative of how they move within their habitats.

Epaulette sharks and the other long-tailed carpet sharks are long and slender. Not surprisingly, axial bending was significantly greater in the tail region of the animals, but it was consistent among gaits (Fig. 7). Many elongate, aquatic vertebrates use traveling waves to propel their bodies through the water during anguilliform and carangiform swimming (Frolich and Biewener 1992; Gillis 1997; Ashley-Ross and Bechtel 2004; Ashley-Ross et al. 2009). A double oscillating system, however, where the amplitude and frequency of the head is decoupled from that of the tail, was only first documented in swimming sharks in 2017 (Hoffmann et al. 2017; Porter et al. 2020). We found that bending increased significantly along the length of the body in a traveling wave toward the tail in the neonate and juvenile epaulette sharks. However, we did not directly compare the head yaw frequency and amplitude to the tailbeat. Likewise, the extent of wavelength decoupling was also not investigated. When Travis (2020) examined axial bending, as quantified between the pectoral and pelvic girdles, no differences were detected when comparing fully and partially submerged sub-adult epaulette sharks. Due to its long, sinewy body, and agile movements within and among the reef matrix, the epaulette shark would be a candidate species for future studies examining oscillating systems.

Based on previous studies, we predicted that axial bending of epaulette sharks should vary among gaits (Frolich and Beiwener 1992; Azizi and Horton 2004; Ashley-Ross et al. 2009; Clardy 2012). Interestingly, we found no differences in axial bending patterns across gaits or between life stages. Because these sharks were completely submerged during aquatic walking, we predicted that a traveling axial wave may provide opposing forces to the water acting on the body (Karakasiliotis et al. 2013; Horner and Jayne 2014). In addition, the flexible, muscular fins push against the substrate, generating propulsive forces during walking gaits (Pridmore 1994; Gillis 1997; Goto et al. 1999; Wilga and Lauder 2001; Willey et al. 2004; Kawano and Blob 2013). Indeed, substrate and incline have impacts on whole body kinematics. Redmann et al. (2020) found that American eel (*Anguilla rostrata*) moved at the greatest velocity on sand where the wave frequency of the body decreased toward the tail. Eel velocity was smallest, and shorter body wavelengths were measured at the steepest inclines. In a comparative study examining three elongate fish species, the species with more exaggerated elongate bodies had more contact with the substrate and moved slower than species with less elongation (Ward et al. 2015). Future studies should incorporate varied levels of submersion as well as substrates with different complexities when quantifying epaulette shark walking gaits.

We hypothesized that velocity and axial bending during aquatic locomotion are innate in epaulette sharks because life stage did not significantly affect our statistical models. In this study, velocity did not vary between neonate and juvenile sharks during submerged walking. We can hypothesize that the epaulette shark paired fins are able to generate relative thrust over these life stages to obtain equal speeds. Being able to immediately and efficiently move upon hatching is the key to survival and innate in most fishes (Leis et al. 1996; Leis et al. 1997; Fisher et al. 2000; Mouritsen et al. 2013). Further experimental work on skeletal morphology and muscle physiology during embryonic development, especially under climate change conditions, is needed to test these ideas in animals, like the epaulette shark, that are capable of both aquatic and terrestrial locomotion (Vilmar and Di Santo 2022). For example, the little skate (*Leucoraja erinacea*) is a batoid that has been used to study walking and punting previously (Lucifora and Vassallo 2002; Macesic and Kajiura 2010; Macesic et al. 2013). Experimental work found that little skates exhibit decreased wing mineralization, and therefore decreased stiffness (Porter et al. 2006; Porter et al. 2007), when embryos are reared under climate change relevant elevated temperatures (Di Santo 2019). If epaulette shark pectoral fins experience decreased mineralization with increased water temperatures, this might impact their ability to utilize walking gaits, especially under the partially submerged conditions they often encounter moving between tidepools and isolated reef flats.

Tail kinematics

The tail of the epaulette shark, like other long-tailed carpet sharks (*Hemiscylliidae)*, is proximally elongated and muscular. In semi-aquatic and aquatic tetrapods, this type of tail, during axial undulation, provides propulsive forces for forward movement. During submerged walking, the tail drags behind the animal acting in two ways. First, it provides deceleration forces. Second, it shifts the center of mass posteriorly, where the highly propulsive forces of the pelvic fins can combat such deceleration (Pridmore 1994; Willey et al. 2004). The tail may also provide stability and support by creating a tripod for the posteriorly shifted center of mass during alternating fin steps. Tripod formation is crucial to the support of body weight of epaulette sharks and tetrapods with sprawling postures on land, and may play a similar stabilizing role in submerged walking (Hildebrand 1980, 1989; Pridmore 1994; Willey et al. 2004).

It would make sense that as the epaulette shark increases its velocity over the three different gaits, it would also increase the amplitude and frequency at which it beats its tail. The epaulette shark tailbeat amplitude model was significant ($P = 0.048$), albeit barely, and while gait was not a significant main effect ($P = 0.094$), there is an increasing trend where tailbeat amplitude increases throughout the gaits from STMW through SWIM (Fig. 6; Table 3). Interestingly, tailbeat frequency was consistent among gaits and did not differ among life stages. At least during these submerged gaits, it appears the neonate and juvenile epaulette sharks move their tails at a consistent frequency, and the tailbeat amplitude increases as they start moving faster, transitioning into the SWIM gait. At greater walking speeds, and ultimately swimming, the increase in tail amplitude suggests that the tail may be used to generate propulsive forces. We suggest that future studies examine the changes in tailbeat frequency and amplitude, and test the forces produced in semi-aquatic or terrestrial environments and the resulting energetic costs.

Duty factor and fin rotation

We expected to observe differences between neonate and juvenile duty factors due to either (1) developmental changes and/or ecological pressures associated with diet shifts, or (2) the differences in body shape hindering the ability of neonates to maintain necessary contact with the tank floor or both. However, we found that the life stage did not significantly affect duty factor (Fig. 8; Table 3). We did find significant differences between fins and gaits. Pelvic fins were in contact with the substrate significantly longer than pectoral fins, and during STMW, pelvic fins were in contact with the substrate approximately 5% longer than during FW. The pelvic fins of epaulette sharks exhibit a significantly greater duty factor during submerged STMW than during FW because slower velocities allow for longer fin contact times to stabilize the shark (Fig. 8). This duty factor difference between aquatic walking could also be relevant to epaulette sharks as they move between tidepools and isolated reef flats. Previous work on sub-adult epaulette sharks found that pectoral fin duty factor was greater when sharks were partially submerged compared to when they were fully submerged (Travis 2020). In that study, the pelvic fins exhibited the opposite pattern: duty factor was greater in the fully submerged sharks. Differences in duty factor and limb coordination are also seen in other vertebrates. For example, in the Californian newt (*Taricha torosa*), movements from land to water resulted in a marked decrease in duty factor, which alters the footfall pattern and the resulting gait used in different environments (Ashley-Ross and Bechtel 2004). Future studies on the epaulette shark should investigate the coordination of the diagonal-sequence gaits and variations in footfall patterns as animals traverse through fully and partially submerged reef structure. When doing this, epaulette sharks will experience fluctuations in environmental conditions (e.g., temperature) that will allow for integration between respiratory physiology and biomechanics. Finally, in addition to emerging as a model for understanding vertebrate biology in future oceans, Pridmore (1994) and Travis (2020) both noted the epaulette shark as a powerful model to study evolutionary transitions from water to land.

We found that epaulette shark pelvic fins protracted and retracted significantly more than the pectoral fins, and gait significantly affected fin rotation (Fig. 9). We predicted that there would be differences between walking and swimming gaits because aquatic walking is typically limb-based (i.e., with coupling of axial undulations), while swimming is axial-based (i.e., minimal or no limb contribution). This results in differences in limb/fin movements between walking and swimming that have been observed in vertebrates that transition between the gaits (Azizi and Horton 2004; Frolich and Biewener 1992; Ashley-Ross and Bechtel 2004; Pace and Gibbs 2009; Kawano and Blob 2013). In sub-adult epaulette sharks, pelvic fins protracted more than pectoral fins during both partially and fully submerged walking (Travis 2020). Pelvic fin protraction in sub-adults was approximately 20° (Travis 2020), while pelvic fin protraction in neonates and juveniles ranged between 24° and 37° (Fig. 9; Table 3). Pelvic fin retraction of partially submerged sub-adults was the greatest (–80°), while pectoral fin retraction of fully submerged walking sharks was the least (∼ –55º; Travis 2020). In contrast, neonate and juvenile epaulette sharks in this study exhibited minimal pectoral fin (i.e., –5° to –7.3°) and pelvic fin (i.e., –17° to –34°) retraction (Fig. 9). Goto et al. (1999) described the pectoral and pelvic fin skeletal and muscular anatomy of epaulette sharks but did not quantify differences between them. They found that epaulette sharks had elongated and basal cartilages and additional musculature when compared to other benthic species. Perhaps, the kinematic differences quantified here and in other studies are due to differences in joint range of motion or muscle physiological cross-sectional area (Pridmore 1994; Travis 2020).

Epaulette sharks, like many organisms, exhibit a definitive ontogenetic shift, when, in this case, neonates utilizing a yolk sac for energy shift to juveniles that actively hunt and forage, total lengths of the animals only ranged from 16 to 21 cm. Examining epaulette sharks, and perhaps other long-tailed carpet shark species, over their entire ontogeny would provide clarity on the impacts of size, gait, and substrate condition on fin range of motion, which are all extremely relevant to this and related species. Interestingly, we found that the pectoral and pelvic fins exhibited different duty factor values (Figs. 8 and 9), which was also true in partially and fully submerged walking sub-adults (Travis 2020). This might suggest that both pairs of fins might be playing a role, though perhaps unequal roles, in producing ground reaction forces and thrust during walking gaits.

We hypothesized that the enlarged abdomen in neonates might also be a source of instability during walking, as it bulges the sides of the body between the pectoral and pelvic fin sets (Fig. 1). While life stage was not a significant main effect when examining protraction, it did significantly affect retraction. Contrary to our hypothesis, neonates showed greater fin retraction than juveniles (Fig. 9).

Emerging techniques, such as three-dimensional video reconstruction of moving morphology (VROMM), could be utilized to investigate the kinematics of axial bending and fin movements in the epaulette shark. VROMM is a methodology that enables point tracking on body surfaces in fully submerged and large volumes, and this technique was adapted from X-ray reconstruction of moving morphology, which utilizes rigid body markers typically implanted on skeletal elements (Brainerd et al. 2010; Knorlein et al. 2016; Hoffmann et al. 2019a). Previous studies have used VROMM to examine pectoral fin rotation in three axes of non-walking species (*Sphyrna tiburo* and *Squalus suckleyi*; Hoffmann et al. 2019a; Hoffmann et al. 2019b). Preliminary data showed that juvenile epaulette sharks experienced pectoral and pelvic fin rotation about three axes, exceeding the rotation previously described in the literature (Hoffmann and Porter, 2019c). In addition to fin rotation, preliminary data showed that fins experienced substantial conformation, or shape change, as they contacted the substrate. Indeed, given the complex reef matrix that epaulette sharks inhabit, future studies could utilize three-dimensional methods, such as VROMM, to study epaulette locomotion across varying substrates, and levels of submersion, and animal sizes.

Conclusions

The epaulette shark is readily able to transition from submerged walking in an aquatic environment to terrestrial walking; in doing so, this species experiences temperature fluctuations and oxygen limitations, among other environmental challenges, and is not supported by the buoyant forces of water. These characteristics make the epaulette shark an appropriate organism to study the range of physiological, morphological, and biomechanical adaptations experienced by coral reef flat species and the traits that will be necessary for them to survive future ocean conditions. Through this study, we advanced the knowledge state regarding submerged locomotion in the epaulette shark and found that kinematics were largely unaffected by changes in body morphology that occur during early life stages. Further investigations on the aquatic and terrestrial gaits used by this species may provide insights into the development of walking locomotion both in and out of water.

The epaulette shark is emerging as a powerful model to study the impacts of anthropogenic stressors, such as climate change, on vertebrate physiology. Elevated temperatures, in particular, have been demonstrated to result in increased metabolic costs as well as mortality over the span of months. The ability of the epaulette shark to move efficiently among micro-habitats under these challenging environmental conditions will directly impact survival. Despite early locomotion and morphology studies by Pridmore (1994) and Goto (1999) in the 1990s, the biomechanics of long-tailed carpet sharks, like the epaulette shark, has remained largely unexplored. This is in stark contrast to the plethora of comparative physiology studies since the start of the 21st century. Throughout this discussion, we have suggested avenues for future research aiming to fully integrate the biomechanics, physiology, and ecological variables, including substrate type and environmental conditions, to name a few, that this species will encounter throughout a tide cycle.

Data Accessibility Statement

The data that support the findings of this study are available at 10.6084/m9.figshare.20480703

Acknowledgments

We would like to thank the Florida Atlantic University Biology Honors Thesis Program, especially Dr Evelyn Frazier and Chelsea Bennice, and the Office of Undergraduate Research and Inquiry for providing mentorship and guidance to the AVH on this undergraduate thesis project. The members of the Florida Atlantic Biomechanics Lab provided support and mentorship throughout this project, especially Drs Sarah Hoffmann, Katherine Galloway, and Danielle Ingle.

Funding

This work was supported, in part, by an Australian Research Council (ARC) Super Science Fellowship, ARC Early Career Discovery Award, and ARC Centre of Excellence for Coral Reef Studies research allocation to J.L.R. We would like to thank The Office of Undergraduate Research and Inquiry Undergraduate Research Grant and Summer Undergraduate Research Fellowships at Florida Atlantic University for providing funding to support this project. This work was supported, in part, by a National Science Foundation Career award [grant number IOS 1941713 to M.E.P.].

References

Allen GR, Erdmann MV, White WT, Fahmi, Dudgeon CL. 2016. Review of the bamboo shark genus *Hemiscyllium* (Orectolobiformes: Hemiscyllidae). J Ocean Sci Found 23:51–97.

Ashley-Ross MA, Bechtel BF. 2004. Kinematics of the transition between aquatic and terrestrial locomotion in the newt *Taricha torosa*. J Exp Biol 207:461–74.

Ashley-Ross MA, Lundin R, Johnson KL. 2009. Kinematics of level terrestrial and underwater walking in the California newt, *Taricha torosa*. J Exp Zool A Ecol Genet Physiol 311A:240–57.

Azizi E, Horton JM. 2004. Patterns of axial and appendicular movements during aquatic walking in the salamander *Siren lacertina*. Zoology 107:111–20.

Ballard WW, Mellinger J, Lechenault H. 1993. A series of normal stages for development of *Scyliorhinus canicula*, the lesser spotted dogfish (Chondrichthyes: Scyliorhinidae). J Exp Biol 267:318–36.

Brainerd EL, Baier DB, Gatesy SM, Hedrick TL, Metzger KA, Gilbert SL, Crisco JJ. 2010. X-ray reconstruction of moving morphology (XROMM): precision, accuracy and applications in comparative biomechanics research. J Exp Zool 313A:262–79.

Carrier DR. 1996. Ontogenetic limits on locomotor performance. Physiol Zool 69:467–88.

Chapman CA, Renshaw GM. 2009. Hematological responses of the grey carpet shark (*Chiloscyllium punctatum*) and the epaulette shark (*Hemiscyllium ocellatum*) to anoxia and re-oxygenation. J Exp Zool A Ecol Genet Physiol 311A:422–38. doi: 10.1002/jez.539. PMID: 19405134.

Clardy TR. 2012. Aquatic and terrestrial locomotion of the rock prickleback, *Xiphister mucosus* (Cottiformes: Zoarcoidei: Stichaeidae). Northwest. Nat. 93:203–10.

Compagno LV, Dando M, Fowler S. 2005. Sharks of the world. New Jersey (NJ): Princeton University Press.

Di Santo V. 2019. Ocean acidification and warming affect skeletal mineralization in a marine fish. Proc Biol Sci 286:20182187.

Dudgeon CL, Corrigan S, Yang L, Allen GR, Erdmann MV, Fahmi Sugeha HY, White WT, Naylor GJP. 2020. Walking, swimming or hitching a ride? Phylogenetics and biogeography of the walking shark genus *Hemiscyllium*. Mar Freshwater Res 71:1107–17.

Fisher R, Bellwood DR, Job SD. 2000. Development of swimming abilities in reef fish larvae. Mar Ecol Prog Ser 202:163–73.

Frolich LM, Biewener AA. 1992. Kinematic and electromyographic analysis of the functional-role of the body axis during terrestrial and aquatic locomotion in the salamander *Ambystoma tigrinum*. J Exp Biol 162:107–30.

Gervais CR, Mourier J, Rummer JL. 2016. Developing in warm water: irregular colouration and patterns of a neonate elasmobranch. Mar Biodivers 46:743–4.

Gervais CR, Nay TJ, Renshaw G, Johansen JL, Steffensen JF, Rummer JL. 2018. Too hot to handle? Using movement to alleviate effects of elevated temperatures in a benthic elasmobranch, *Hemiscyllium ocellatum*. Mar Biol 165:162.

Gillis GB. 1997. Anguilliform locomotion in an elongate salamander (*Siren intermedia*): effects of speed on axial undulatory movements. J Exp Biol 200:767–84.

Goto T, Nishida K, Nakaya K. 1999. Internal morphology and function of paired fins in the epaulette shark, *Hemiscyllium ocellatum*. Ichthyol Res 46:281–7.

Harahush BK, Fischer ABP, Collin S. 2007. Captive breeding and embryonic development of *Chiloscyllium punctatum* Muller and Henle, 1838 (Elasmobranchii: Hemiscyllidae). J Fish Biol 71:1007–22.

Harborne AR. 2013. The ecology, behaviour and physiology of fishes on coral reef flats, and the potential impacts of climate change, J Fish Biol 83:417–47.

Heinrich DDU, Rummer JL, Morash AJ, Watson S-A, Simpfendorfer CA, Heupel MR, Munday PL. 2014. A product of its environment: the epaulette shark (*Hemiscyllium ocellatum*) exhibits physiological tolerance to elevated environmental CO2. Conservation Physiology 2: cou047.

Heinrich DDU, Watson S-A, Rummer JL, Brandl SJ, Simpfendorfer CA, Heupel MR, Munday PL. 2014. Foraging behaviour of the epaulette shark *Hemiscyllium ocellatum* is not affected by elevated CO_2. ICES J Mar Sci 71:528–36.

Herrel A, Gibb AC. 2006. Ontogeny of performance in vertebrates. Physiol Biochem Zool 79:1–6.

Heupel MR, Bennett MB. 1998. Observations on the diet and feeding habits of the epaulette shark, *Hemiscyllium ocellatum* (Bonnaterre), on Heron Island Reef, Great Barrier Reef, Australia. Mar Freshwater Res 49:753–6.

Heupel MR, Bennett MB. 2007. Estimating abundance of reef-dwelling sharks: a case study of the epaulette shark, *Hemiscyllium ocellatum* (Elasmobranchii : Hemiscyllidae). Pac Sci 61:383–94.

Hildebrand M. 1980. The adaptive significance of tetrapod gait selection. Am Zool 20:255–67.

Hildebrand M. 1989. The quadrupedal gaits of vertebrates, Bioscience 39:766–75.

Hoffmann SL, Warren SM, Porter ME. 2017. Regional variation in undulatory kinematics of two hammerhead species: the bonnethead (*Sphyrna tiburo*) and the scalloped hammerhead (*Sphyrna lewini*). J Exp Biol 220:3336–43.

Hoffmann SL, Donatelli CM, Leigh SC, Brainerd EL, Porter ME. 2019a. Three-dimensional movements of the pectoral fin during yaw turns in the Pacific spiny dogfish, *Squalus suckleyi*. Biol Open 8:bio037291. doi: https://doi.org/10.1242/bio.037291

Hoffmann SL, Porter ME. 2019b. Body and pectoral fin kinematics during routine yaw turning in bonnethead sharks (*Sphyrna tiburo*). Integr org biol 1:obz014, https://doi.org/10.1093/iob/obz014

Hoffmann SL, Porter ME. 2019c. Three-dimensional kinematics of underwater walking in the epaulette shark. Society of Integrative and Comparative Biology. 2019c Annual Meeting Abstracts 59:336.

Horner AM, Jayne BC. 2014. Lungfish axial muscle function and the vertebrate water to land transition.PLoS One 9:e96516.

Horning M, Trillmich F. 1997. Ontogeny of diving behaviour in the Galapagos fur seal. Behaviour 134:1211–57.

Karakasiliotis K, Schilling N, Cabelguen J-M, Ijspeert AJ. 2013. Where are we in understanding salamander locomotion: biological and robotic perspectives on kinematics. Biol Cybern 107:529–44.

Kawano SM, Blob RW. 2013. Propulsive forces of mudskipper fins and salamander limbs during terrestrial locomotion: implications for the invasion of land. Integr Comp Biol 53:283–94.

Kirkton SD, Harrison OF. 2006. Ontogeny of locomotory behaviour in the American locust, *Schistocerca americana*: from marathoner to broad jumper. Anim Behav 71:925–31.

Knörlein BJ, Baier DB, Gatesy SM, Laurence-Chasen JD, Brainerd EL. 2016. Validation of XMALab software for marker-based XROMM. J Exp Biol 219:3701–11.

Leis JM, Carson-Ewart BM. 1997. *In situ* swimming speeds of the late pelagic larvae of some Indo-Pacific coral-reef fishes. Mar Ecol Prog Ser 159:165–74.

Leis JM, Sweatman HP, Reader SE. 1996. What the pelagic stages of coral reef fishes are doing out in blue water: daytime field observations of larval behavioural capabilities. Mar Freshwater Res 47:401–11.

Long JH, Jr., Porter ME, Root RG, Liew CW. 2010. Go refigure: how fish change shape as they swim and evolve. Integr Comp Biol 50:1120–39.

Lopes AR, Sampaio E, Santos C, Couto A, Pegado MR, Diniz M, Munday PL, Rummer JL, Rosa R. 2018. Absence of cellular damage in tropical newly-hatched sharks (*Chiloscyllium plagiosum*) under ocean acidification conditions. Cell Stress Chaperones 23:837–46.

Lucifora LO, Vassallo AI. 2002. Walking in skates (Chondrichthyes, Rajidae): anatomy, behaviour and analogies to tetrapod locomotion, Biol J Linn Soc 77:35–41.

Macesic LJ, Kajiura SM. 2010. Comparative punting kinematics and pelvic fin musculature of benthic batoids. J Morphol 271:1219–28.

Macesic LJ, Mulvaney D, Blevins EL. 2013. Synchronized swimming: coordination of pelvic and pectoral fins during augmented punting by the freshwater stingray *Potamotrygon orbignyi*. Zoology 116:144–50.

Mouritsen H, Atema J, Kingsford MJ, Gerlach G. 2013. Sun compass orientation helps coral reef fish larvae return to their natal reef. PLoS One 8:e66039.

Müller. 1848. Fossile Fische. Reisse in den äusserstem Norden und Osten Siberiens während der Jahr 1843-44. Herausgegeben von A. Th. V. Moddendorf, I.

Nay TJ, Longbottom RJ, Gervais CR, Johansen JL, Steffensen JF, Rummer JL, Hoey AS. 2020. Regulate or tolerate: thermal strategy of a coral reef flat resident, the epaulette shark, *Hemiscyllium ocellatum*. J Fish Biol 98:723–32.

Pace CM, Gibb AC. 2009. Mudskipper pectoral fin kinematics in aquatic and terrestrial environments. J Exp Biol 212:2279–86.

Payne EJ, Rufo KS. 2012. Husbandry and growth rates of neonate epaulette sharks, *Hemiscyllium ocellatum* in captivity. Zoo Biol 31:718–24.

Pegado MR, Santos C, Couto A, Pinto E, Lopes AR, Diniz M, Rosa R. 2018. . Mar Freshw Behav Physiol 51:347–57.

Pegado MR, Santos CP, Pimentel M, Cyrne R, Maulvaut AL, Raffoul D, Diniz M, Bispo R, Rosa R.2020. Effects of elevated carbon dioxide on hematological parameters of a temperate catshark. J Exp Zool A Ecol Integr Physiol 333:126–32.

Pereira Santos C, Sampaio E, Pereira B, Pegado MR, Borges FO, Wheeler C, Bouyoucos I, Rummer J, Frazão Santos C, Rosa R. 2021. Elasmobranch responses to experimental warming, acidification, and oxygen loss - a meta-analysis. Front Mar Sci 8:1380.

Porter MR, Beltrán JL, Koob TJ, Summers AP. 2006. Material properties and biochemical composition of mineralized vertebral cartilage in seven elasmobranch species (Chondrichthyes). J Exp Biol 209:2920–2928.

Porter ME, Koob TJ, Summers AP. 2007. The contribution of mineral to the material properties of vertebral cartilage from the smooth-hound shark *Mustelus californicus*. J Exp Biol 210:3319–3327.

Porter ME, Roque C, Long JH, Jr. 2009. Turning maneuvers in sharks: predicting body curvature from vertebral morphology. J Morphol 270:954–965.

Porter ME, Rogue CM, Jr Long JH. 2011. Body form and posture mediate angular head speed during yaw turning in sharks. Zoology 114:348–59.

Porter ME, Ruddy C, Kajiura SM. 2020. Volitional swimming kinematics of blacktip sharks, *Carcharhinus limbatus*, in the wild. Drones 4:78. https://doi.org/10.3390/drones4040078

Pridmore PA. 1994. Submerged walking in the epaulette shark *Hemiscyllium ocellatum* (Hemiscyllidae) and its implications for locomotion in rhipidistian fishes and early tetrapod.Zoology 98:278–97.

Raoult V, Tosetto L, Williamson J. 2018. Drone-based high-resolution tracking of aquatic vertebrates. Drones 2: 37.

Redmann E, Sheikh A, Alqahtani A, McCarty-Glenn M, Syed S, Mehta RS, Ward AB. 2020. Terrestrial locomotion in American eels (*Anguilla rostrata*): how substrate and incline affect movement patterns. Integr Comp Biol 60:180–9.

Reilly SM, McElroy EJ, Odum RA, Hornyak VA. 2006. Tuataras and salamanders show that walking and running mechanics are ancient features of tetrapod locomotion. Proc R Soc Lond B Biol Sci 273:1563–8.

Rodda KR, Seymour RS. 2008. Functional morphology of embryonic development in the Port Jackson shark *Heterodontus portusjacksoni* (Meyer). J Fish Biol 72:961–84.

Rosa R, Rummer JL, Munday PL. 2017. Biological responses of sharks to ocean acidification. Biol Lett 13:20160796. doi: 10.1098/rsbl.2016.0796

Rummer JL, Bouyoucos IA, Wheeler C, Santos CP, Rosa R. 2022. Climate change and sharks. Vol. 25In: Carrier JC, Simpfendorfer CA, Heithaus MR, Yopak KE (eds.), Biology of sharks and their relatives, Third edition. CRC Press. p. 840.

Rosenblum HG, Long JH, Jr, Porter ME. 2011. Sink and swim: kinematic evidence for axial undulatory and lifting-body mechanisms in negatively-buoyant electric rays (*Narcine brasiliensis*). J Exp Biol 214:2935–48.

Routley MH, Nilsson GE, Renshaw GM. 2002. Exposure to hypoxia primes the respiratory and metabolic responses of the epaulette shark to progressive hypoxia. Comp Biochem Physiol A: Mol Integr Physiol 131:313–21.

Stewart JR, Castillo RE. 1984. Nutritional provision of the yolk of two species of viviparous peptiles. Physiol Zool 57: 377–83.

Travis KG. 2020.Comparative biomechanics of submerged and partially emerged walking in the epaulette shark (*Hemiscyllium ocellatum*).California (CA): California State University. p.66. Master's thesis.

Vilmar M, Di Santo V. 2022. Swimming performance of sharks and rays under climate change. Rev Fish Biol Fish 32:765–81.

Ward AB, Costa A, Monroe SL, Aluck RJ, Mehta RS. 2015. Locomotion in elongate fishes: a contact sport. Zoology 118: 312–9.

West JG, Carter S. 1990. Observations on the development and growth of the epaulette shark *Hemicyllium ocellatum* (Bonnaterre) in captivity, J Aquac Res Dev 5:111–7.

Wheeler CR, Gervais CR, Johnson MS, Vance S, Rosa R, Mandelman JW, Rummer JL. 2020. Anthropogenic stressors influence reproduction and development in elasmobranch fishes. Rev Fish Biol Fish 30:373–86.

Wheeler CR, Rummer JL, Bailey B, Lockwood J, Vance S, Mandelman JW. 2021. Future thermal regimes for epaulette sharks (*Hemiscyllium ocellatum*): growth and metabolic performance cease to be optimal. Sci Rep 11:1–12.

Wilga CD, Lauder GV. 2001. Functional morphology of the pectoral fins in bamboo sharks, *Chiloscyllium plagiosum*: Benthic vs. pelagic station-holding, J Morphol 249:195–209.

Willey JS, Biknevicius AR, Reilly SM, Earls KD. 2004. The tale of the tail: limb function and locomotor mechanics in *Alligator mississippiensis*. J Exp Biol 207:553–63.